

SUPERMASSIVE BLACK HOLES IN INACTIVE GALAXIES¹

John Kormendy² and Luis C. Ho³

1. INTRODUCTION

Several billion years after the Big Bang, the Universe went through a “quasar era” when high-energy active galactic nuclei (AGNs) were more than 10,000 times as numerous as they are now. Quasars must then have been standard equipment in most large galaxies. Since that time, AGNs have been dying out. Now quasars are exceedingly rare, and even medium-luminosity AGNs such as Seyfert galaxies are uncommon. The only activity that still occurs in many galaxies is weak. A paradigm for what powers this activity is well established through the observations and theoretical arguments that are outlined in the previous article. AGN engines are believed to be supermassive black holes (BHs) that accrete gas and stars and so transform gravitational potential energy into radiation. Expected BH masses are $M_{\bullet} \sim 10^6 - 10^{9.5} M_{\odot}$. A wide array of phenomena can be understood within this picture. But the subject has had an outstanding problem: there was no dynamical evidence that BHs exist. The search for BHs has therefore become one of the hottest topics in extragalactic astronomy.

Since most quasars have switched off, dim or dead engines – starving black holes – should be hiding in many nearby galaxies. This means that the BH search need not be confined to the active galaxies that motivated it. In fact, definitive conclusions are much more likely if we observe objects in which we do not, as Alan Dressler has said, “have a searchlight in our eyes.” Also, it was necessary to start with the nearest galaxies, because only then could we see close enough to the center so that the BH dominates the dynamics. Since AGNs are rare, nearby galaxies are not particularly active. For these reasons, it is no surprise that the search first succeeded in nearby, inactive galaxies.

This article discusses stellar dynamical evidence for BHs in inactive and weakly active galaxies. Stellar motions are a particularly reliable way to measure masses, because stars cannot be pushed around by nongravitational forces. The price is extra complication in the analysis: the dynamics are collisionless, so random velocities can be different in different directions. This is impossible in a collisional gas. As we shall see, much effort has gone into making sure that unrecognized velocity anisotropy does not lead to systematic errors in mass measurements.

Dynamical evidence for central dark objects has been published for 17 galaxies. With the *Hubble Space Telescope* (*HST*) pursuing the search, the number of detections is growing rapidly. Already we can ask demographic questions. Two main results have emerged. First, the numbers and masses of central dark objects are broadly consistent with predictions based on quasar energetics. Second, the central dark mass correlates with the mass of the elliptical-galaxy-like

¹ To appear in *Encyclopedia of Astronomy and Astrophysics*

² Department of Astronomy, RLM 15.308, University of Texas, Austin, TX 78712-1083

³ Carnegie Observatories, 813 Santa Barbara St., Pasadena, CA 91101-1292

“bulge” component of galaxies. What is less secure is the conclusion that the central dark objects must be BHs and not (for example) dense clusters of brown dwarf stars or stellar remnants. Rigorous arguments against such alternatives are available for only two galaxies. Nevertheless, these two objects and the evidence for dark masses at the centers of almost all galaxies that have been observed are taken as strong evidence that the AGN paradigm is essentially correct.

2. DEAD QUASAR ENGINES IN NEARBY GALAXIES

The qualitative discussion of the previous section can be turned into a quantitative estimate for M_\bullet as follows. The quasar population produces an integrated comoving energy density of

$$u = \int_0^\infty \int_0^\infty \Phi(L, z) L dL \frac{dt}{dz} dz = 1.3 \times 10^{-15} \text{ erg cm}^{-3}, \quad (1)$$

where $\Phi(L, z)$ is the comoving density of quasars of luminosity L at redshift z and t is cosmic time. For a radiative energy conversion efficiency of ϵ , the equivalent present-day mass density is $\rho_u = u/(\epsilon c^2) = 2.2 \times 10^4 \epsilon^{-1} \text{ M}_\odot \text{ Mpc}^{-3}$. Comparison of ρ_u with the overall galaxy luminosity density, $\rho_g \simeq 1.4 \times 10^8 h \text{ L}_\odot \text{ Mpc}^{-3}$, where the Hubble constant is $H_0 = 100 h \text{ km s}^{-1} \text{ Mpc}^{-1}$, implies that a typical nearby bright galaxy (luminosity $L^* \simeq 10^{10} h^{-2} \text{ L}_\odot$) should contain a dead quasar of mass $M_\bullet \sim 1.6 \times 10^6 \epsilon^{-1} h^{-3} \text{ M}_\odot$. Accretion onto a BH is expected to produce energy with an efficiency of $\epsilon \sim 0.1$, and the best estimate of h is 0.71 ± 0.06 . Therefore the typical BH should have a mass of $\sim 10^{7.7} \text{ M}_\odot$. BHs in dwarf ellipticals should have masses of $\sim 10^6 \text{ M}_\odot$.

In fact, the brightest quasars must have had much higher masses. A BH cannot accrete arbitrarily large amounts of mass to produce arbitrarily high luminosities. For a given M_\bullet , there is a maximum accretion rate above which the radiation pressure from the resulting high luminosity blows away the accreting matter. This “Eddington limit” is discussed in the preceding article. Eddington luminosities of $L \sim 10^{47} \text{ erg s}^{-1} \sim 10^{14} \text{ L}_\odot$ require BHs of mass $M_\bullet \gtrsim 10^9 \text{ M}_\odot$. These arguments define the parameter range of interest: $M_\bullet \sim 10^6$ to $10^{9.5} \text{ M}_\odot$. The highest-mass BHs are likely to be rare, but low-mass objects should be ubiquitous. Are they?

3. STELLAR DYNAMICAL SEARCHES FOR CENTRAL DARK OBJECTS

The answer appears to be “yes”. The majority of detections on which this conclusion is based are stellar-dynamical. However, finding BHs is not equally easy in all galaxies. This results in important selection effects that need to be understood for demographic studies. Therefore we begin with a discussion of techniques. We then give three examples that highlight important aspects of the search. NGC 3115 is a particularly clean detection that illustrates the historical development of the search. M31 is one of the nearest galaxies and contains a new astrophysical phenomenon connected with BHs. Finally, the strongest case that the central mass is a BH and not a dark cluster of stars or stellar remnants is the one in our own Galaxy.

3.1 Stellar Dynamical Mass Measurement

Dynamical mass measurement is conceptually simple. If random motions are small, as they are in a gas, then the mass $M(r)$ within radius r is $M(r) = V^2 r / G$. Here V is the rotation

velocity and G is the gravitational constant. In stellar systems, some dynamical support comes from random motions, so $M(r)$ depends also on the velocity dispersion σ . The measurement technique is best described in the idealized case of spherical symmetry and a velocity ellipsoid that points at the center. Then the first velocity moment of the collisionless Boltzmann equation gives

$$M(r) = \frac{V^2 r}{G} + \frac{\sigma_r^2 r}{G} \left[-\frac{d \ln \nu}{d \ln r} - \frac{d \ln \sigma_r^2}{d \ln r} - \left(1 - \frac{\sigma_\theta^2}{\sigma_r^2}\right) - \left(1 - \frac{\sigma_\phi^2}{\sigma_r^2}\right) \right]. \quad (2)$$

Here σ_r , σ_θ , and σ_ϕ are the radial and azimuthal components of the velocity dispersion. The density ν is not the total mass density ρ ; it is the density of the luminous tracer population whose kinematics we measure. We never see ρ , because the stars that contribute most of the light contribute almost none of the mass. Therefore we assume that $\nu(r) \propto$ volume brightness. All quantities in Equation 2 are unprojected. We observe brightnesses and velocities after projection and blurring by a point-spread function (PSF). Information is lost in both processes. Several techniques have been developed to derive unprojected quantities that agree with the observations after projection and PSF convolution. From these, we derive the mass distribution $M(r)$ and compare it to the light distribution $L(r)$. If $M/L(r)$ rises rapidly as $r \rightarrow 0$, then we have found a central dark object.

There is one tricky problem with this analysis, and it follows directly from Equation 2. Rotation and random motions contribute similarly to $M(r)$, but the $\sigma^2 r/G$ term is multiplied by a factor that depends on the velocity anisotropy and that can be less than 1. Galaxy formation can easily produce a radial velocity dispersion σ_r that is larger than the azimuthal components σ_θ and σ_ϕ . Then the third and fourth terms inside the brackets in Equation 2 are negative; they can be as small as -1 each. In fact, they can largely cancel the first two terms, because the second term cannot be larger than $+1$, and the first is $\simeq 1$ in many galaxies. This explains why *ad hoc* anisotropic models have been so successful in explaining the kinematics of giant ellipticals without BHs. But how anisotropic are the galaxies?

Much effort has gone into finding the answer. The most powerful technique is to construct self-consistent dynamical models in which the density distribution is the linear combination $\rho = \sum N_i \rho_i$ of the density distributions ρ_i of the individual orbits that are allowed by the gravitational potential. First the potential is estimated from the light distribution. Orbits of various energies and angular momenta are then calculated to construct a library of time-averaged density distributions ρ_i . Finally, orbit occupation numbers N_i are derived so that the projected and PSF-convolved model agrees with the observed kinematics. Some authors also maximize $\sum N_i \ln N_i$, which is analogous to an entropy. These procedures allow the stellar distribution function to be as anisotropic as it likes in order (e.g.) to try to explain the observations without a BH. In the end, such models show that real galaxies are not extremely anisotropic. That is, they do not take advantage of all the degrees of freedom that the physics would allow. However, this is not something that one could take for granted. Because the degree of anisotropy depends on galaxy luminosity, almost all BH detections in bulges and low-luminosity ellipticals (which are nearly isotropic) are based on stellar dynamics, and almost all BH detections in giant ellipticals (which are more anisotropic) are based on gas dynamics.

3.2 NGC 3115: $M_{\bullet} \simeq 10^{9.0 \pm 0.3} M_{\odot}$

One of the best stellar-dynamical BH cases is the prototypical S0 galaxy NGC 3115 (Fig. 1). It is especially suitable for the BH search because it is very symmetrical and almost exactly edge-on. NGC 3115 provides a good illustration of how the BH search makes progress. Unlike some discoveries, finding a supermassive BH is rarely a unique event. Rather, an initial dynamical case for a central dark object gets stronger as observations improve. Eventually, the case becomes definitive. This has happened in NGC 3115 through the study of the central star cluster – a tiny, dense cusp of stars like those expected around a BH (Figure 1). Later, still better observations may accomplish the next step, which is to strengthen astrophysical constraints enough so that all plausible BH alternatives (clusters of dark stars) are eliminated. This has happened for our Galaxy (§ 3.4) but not yet for NGC 3115.

The kinematics of NGC 3115 show the signature of a central dark object (Fig. 2). The original detection was based on the blue crosses. Already at resolution $\sigma_* = 0''.44$, the central kinematic gradients are steep. The apparent central dispersion, $\sigma \simeq 300 \text{ km s}^{-1}$, is much higher than normal for a galaxy of absolute magnitude $M_B = -20.0$. Therefore, isotropic dynamical models imply that NGC 3115 contains a dark mass $M_{\bullet} \simeq 10^{9 \pm 0.3} M_{\odot}$. Maximally anisotropic models allow smaller masses, $M_{\bullet} \sim 10^8 M_{\odot}$, but isotropy is more likely given the rapid rotation.

Since that time, two generations of improved observations have become available. The green points in Figure 2 were obtained with the Subarcsecond Imaging Spectrograph (SIS) and the Canada-France-Hawaii Telescope (CFHT). This incorporates tip-tilt optics to improve the atmospheric PSF. The observations with the *HST* Faint Object Spectrograph (FOS) have still higher resolution. If the BH detection is correct, then the apparent rotation and dispersion profiles should look steeper when they are observed at higher resolution. This is exactly what is observed. If the original dynamical models are “reobserved” at the improved resolution, the ones that agree with the new data have $M_{\bullet} = (1 \text{ to } 2) \times 10^9 M_{\odot}$.



Figure 1. *HST* WFPC2 images of NGC 3115. The left panel shows a color image made from 1050 s *V*- and *I*-band images. The right panel shows a model of the nuclear disk. The center panel shows the difference; it emphasizes the compact nuclear star cluster. Brightness is proportional to the square root of intensity. All panels are $11''.6$ square. [This figure is taken from Kormendy *et al.* 1996, *Astrophys. J. Lett.*, **459**, L57.]

Finally, a definitive detection is provided by the *HST* observations of the nuclear star cluster. Its true velocity dispersion is underestimated in Figure 2, because the projected value includes bulge light from in front of and behind the center. When this light is subtracted, the velocity dispersion of the nuclear cluster proves to be $\sigma = 600 \pm 37 \text{ km s}^{-1}$. This is the highest dispersion measured in any galactic center. The velocity of escape from the nucleus would be much smaller, $V_{\text{esc}} \simeq 352 \text{ km s}^{-1}$, if it consisted only of stars. Without extra mass to bind it, the cluster would fling itself apart in $\sim 2 \times 10^4 \text{ yr}$. Independent of any velocity anisotropy, the nucleus must contain an unseen object of mass $M_{\bullet} \simeq 10^9 M_{\odot}$. This is consistent with the modeling results. The dark object is more than 25 times as massive as the visible star cluster. We know of no way to make a star cluster that is so nearly dark, especially without overenriching the visible stars with heavy elements. The most plausible explanation is a BH. This would easily have been massive enough to power a quasar.

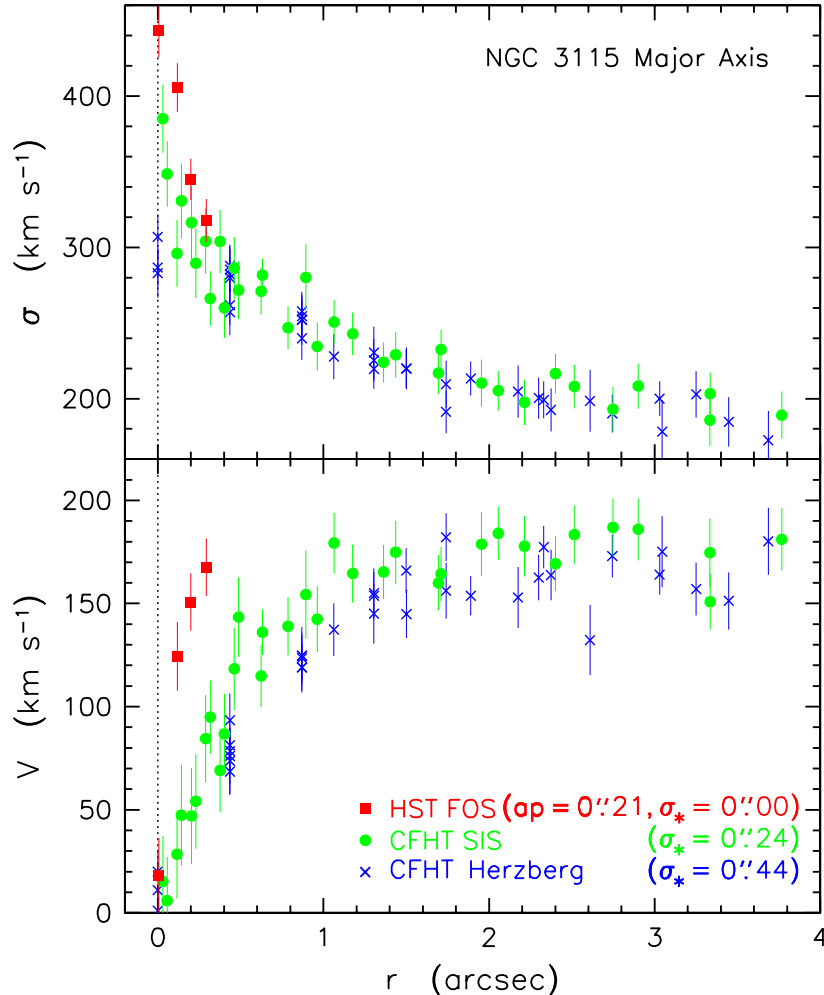


Figure 2. Rotation velocities (lower panel) and velocity dispersions (upper panel) along the major axis of NGC 3115 as observed at three different spatial resolutions. Resolution σ_* is the Gaussian dispersion radius of the PSF; in the case of the *HST* observations, this is negligible compared to the aperture size of $0''.21$. [This figure is adapted from Kormendy *et al.* 1996, *Astrophys. J. Lett.*, **459**, L57.]

3.3 M 31: $M_{\bullet} \simeq 3 \times 10^7 M_{\odot}$

M 31 is the highest-luminosity galaxy in the Local Group. At a distance of 0.77 Mpc, it is the nearest giant galaxy outside our own. It can therefore be studied in unusual detail.

M 31 contains the nearest example of a nuclear star cluster embedded in a normal bulge. When examined with *HST*, the nucleus appears double (Figure 3). This is very surprising. At a separation of $2r = 0''.49 = 1.7$ pc, a relative velocity of 200 km s^{-1} implies a circular orbit period of 50,000 yr. If the nucleus consisted of two star clusters in orbit around each other, as Fig. 3 might suggest, then dynamical friction would make them merge within a few orbital times. Therefore it is unlikely that the simplest possible explanation is correct: we are not observing the last stages of the digestion of an accreted companion galaxy.

The nucleus rotates rapidly and has a steep velocity dispersion gradient (Figure 3). Dynamical analysis shows that M 31 contains a central dark mass $M_{\bullet} \simeq 3 \times 10^7 M_{\odot}$. The possible effects of velocity anisotropy have been checked and provide no escape. Furthermore, the asymmetry provides an almost independent check of the BH mass, as follows.

The top panel of Figure 3 shows the *HST* image at the same scale as and registered in position with the kinematics. It shows that the dispersion peak is approximately centered on the fainter nucleus. In fact, it is centered almost exactly on a cluster of blue stars that is embedded in this nucleus. This suggests that the BH is in the blue cluster. This hypothesis can be tested by finding the center of mass of the asymmetric distribution of starlight plus a dark object in the blue cluster. The mass-to-light ratio of the stars is provided by dynamical models of the bulge at larger radii. If the galaxy is in equilibrium, then the center of mass should coincide with the center of the bulge. It does, provided that $M_{\bullet} \simeq 3 \times 10^7 M_{\odot}$. Remarkably, the same BH mass explains the kinematics and the asymmetry of the nucleus.

An explanation of the mysterious double nucleus has been proposed by Scott Tremaine. He suggests that both nuclei are part of a single eccentric disk of stars. The brighter nucleus is farther from the barycenter; it results from the lingering of stars near the apocenters of very elongated orbits. The fainter nucleus is produced by an increase in disk density toward the center. The model depends on the presence of a BH to make the potential almost Keplerian; then the alignment of orbits in the eccentric disk may be maintained by the disk's self-gravity. Tremaine's model was developed to explain the photometric and kinematic asymmetries as seen at resolution $\sigma_* \simeq 0''.5$. It is also consistent with the data in Figure 3 ($\sigma_* \simeq 0''.27$). The high velocity dispersion near the BH, the low dispersion in the offcenter nucleus, and especially the asymmetric rotation curve are signatures of the eccentric, aligned orbits.

Most recently, spectroscopy of M 31 has been obtained with the *HST* Faint Object Camera. This improves the spatial resolution by an additional factor of ~ 5 . At this resolution, there is a $0''.25$ wide region centered on the faint nucleus in which the velocity dispersion is $440 \pm 70 \text{ km s}^{-1}$. This is further confirmation of the existence and location of the BH.

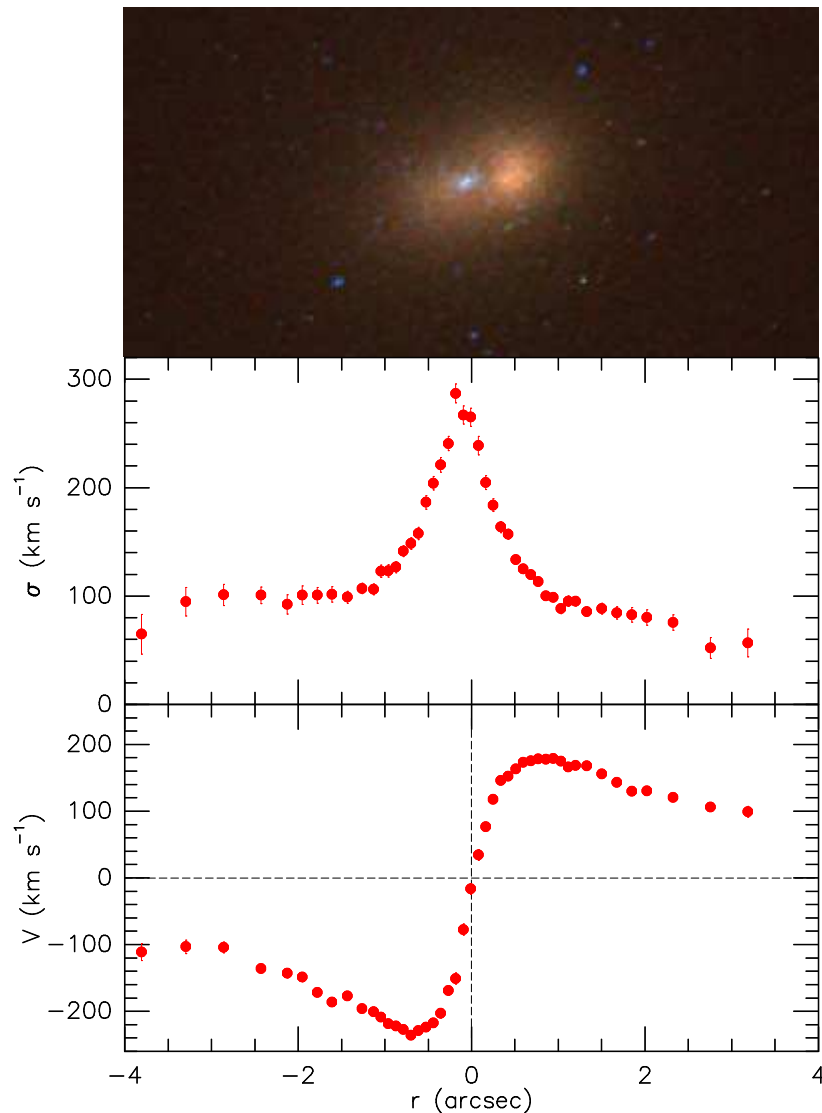


Figure 3. (*top*) *HST* WFPC2 color image of M31 constructed from *I*-, *V*- and 3000 Å-band, PSF-deconvolved images obtained by Lauer *et al.* (1998, *Astron. J.*, **116**, 2263). The scale is 0''.0228 pixel⁻¹. (*bottom and middle*) Rotation curve $V(r)$ and velocity dispersion profile $\sigma(r)$ of the nucleus with foreground bulge light subtracted. The symmetry point of the rotation curve and the sharp dispersion peak suggest that the BH is in the blue star cluster embedded in the left brightness peak. [This figure is adapted from Kormendy & Bender 1999, *Astrophys. J.*, **522**, 772.]

We do not know whether the double nucleus is the cause or an effect of the offcenter BH. However, offcenter BHs are an inevitable consequence of hierarchical structure formation and galaxy mergers. If most large galaxies contain BHs, then mergers produce binary BHs and, in three-body encounters, BH ejections with recoil. How much offset we see, and indeed whether we see two BHs or one or none at all, depend on the relative rates of mergers, dynamical friction, and binary orbit decay. Offcenter BHs may have much to tell us about these and other processes. Already there is evidence in NGC 4486B for a second double nucleus containing a BH.

3.4 Our Galaxy: $M_{\bullet} \simeq (2.9 \pm 0.4) \times 10^6 M_{\odot}$

Our Galaxy has long been known to contain the exceedingly compact radio source Sgr A*. Interferometry gives its diameter as $63 r_s$ by less than $17 r_s$, where $r_s = 0.06 \text{ AU} = 8.6 \times 10^{11} \text{ cm}$ is the Schwarzschild radius of a $2.9 \times 10^6 M_{\odot}$ BH. It is easy to be impressed by the small size. But as an AGN, Sgr A* is feeble: its radio luminosity is only $10^{34} \text{ erg s}^{-1} \simeq 10^{0.4} L_{\odot}$. The infrared and high-energy luminosities are higher, but there is no compelling need for a BH on energetic grounds. To find out whether the Galaxy contains a BH, we need dynamical evidence.

Getting it has not been easy. Our Galactic disk, which we see in the sky as the Milky Way, contains enough dust to block all but $\sim 10^{-14}$ of the optical light from the Galactic center. Measurements of the region around Sgr A* had to await the development of infrared detectors. Much of the infrared radiation is in turn absorbed by the Earth's atmosphere, but there is a useful transmission window at $2.2 \mu\text{m}$ wavelength. Here the extinction toward the Galactic center is a factor of ~ 20 . This is large but manageable. Early infrared measurements showed a rotation velocity of $V \simeq 100 \text{ km s}^{-1}$ and a small rise in velocity dispersion to $\sim 120 \text{ km s}^{-1}$ at the center. These were best fit with a BH of mass $M_{\bullet} \sim 10^6 M_{\odot}$, but the evidence was not very strong. Since then, a series of spectacular technical advances have made it possible to probe closer and closer to the center. As a result, the strongest case for a BH in any galaxy is now our own.

Most remarkably, two independent groups led by Reinhard Genzel and Andrea Ghez have used speckle imaging to measure proper motions – the velocity components perpendicular to the line of sight – in a cluster of stars at radii $r \lesssim 0''.5 \simeq 0.02 \text{ pc}$ from Sgr A* (Figure 4). When combined with complementary measurements at larger radii, the result is that the one-dimensional velocity dispersion increases smoothly to $420 \pm 60 \text{ km s}^{-1}$ at $r \simeq 0.01 \text{ pc}$. Stars at this radius revolve around the Galactic center in a human lifetime! The mass $M(r)$ inside radius r is shown in Figure 5. Outside a few pc, the mass distribution is dominated by stars, but as $r \rightarrow 0$, $M(r)$ flattens to a constant, $M_{\bullet} = (2.9 \pm 0.4) \times 10^6 M_{\odot}$. Velocity anisotropy is not an uncertainty; it is measured directly and found to be small. The largest dark cluster that is consistent with these data would have a central density of $4 \times 10^{12} M_{\odot} \text{ pc}^{-3}$. This is inconsistent with astrophysical constraints (§ 5). Therefore, if the dark object is not a BH, the alternative would have to be comparably exotic. It is prudent to note that rigorous proof of a BH requires that we spatially resolve relativistic velocities near the Schwarzschild radius. This is not yet feasible. But the case for a BH in our own Galaxy is now very compelling.

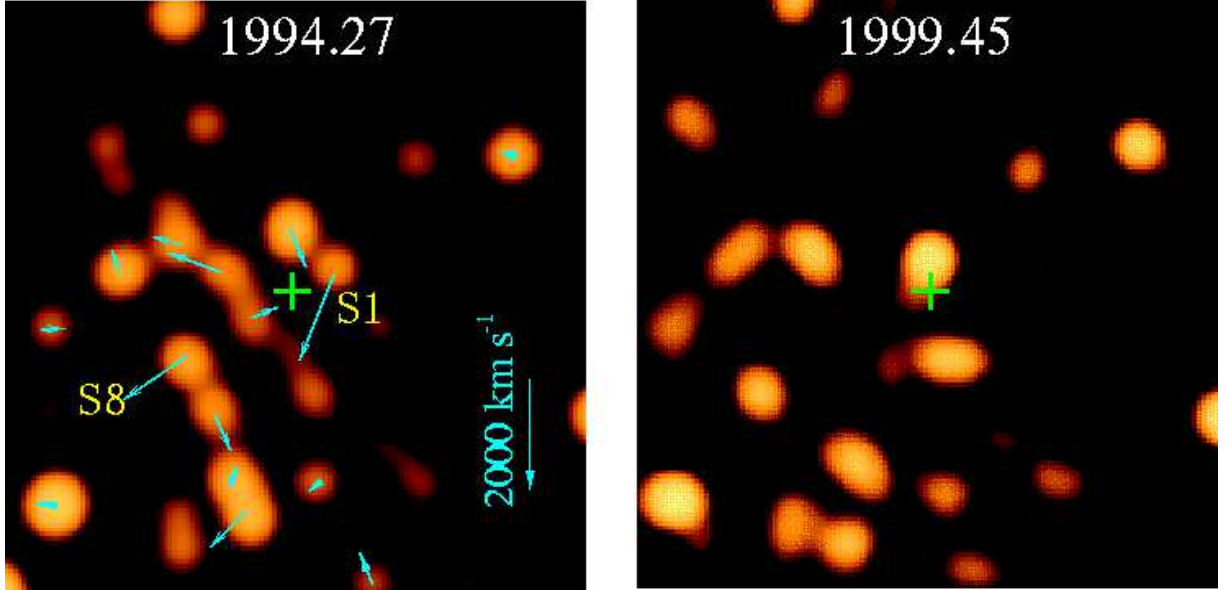


Figure 4. Images of the star cluster surrounding Sgr A* (green cross) at the epochs indicated. The arrows in the left frame show approximately where the stars have moved in the right frame. Star S1 has a total proper motion of $\sim 1600 \text{ km s}^{-1}$. [This figure is updated from Eckart & Genzel 1997, *M. N. R. A. S.*, **284**, 576 and was kindly provided by A. Eckart.]

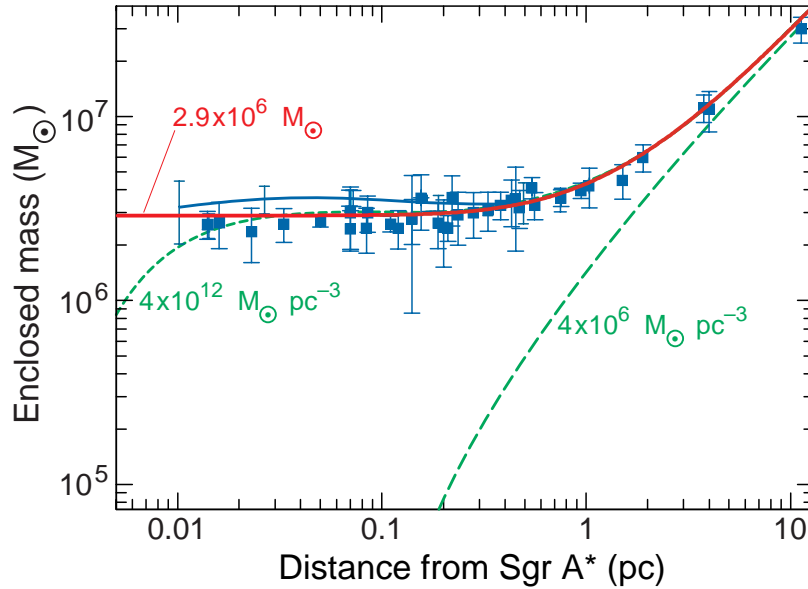


Figure 5. Mass distribution implied by proper motion and radial velocity measurements (blue points and curve). Long dashes (green) show the mass distribution of stars if the infrared mass-to-light ratio is 2. The red curve represents the stars plus a point mass $M_{\bullet} = 2.9 \times 10^6 M_{\odot}$. Short green dashes provide an estimate of how non-pointlike the dark mass could be: its χ^2 value is 1σ worse than the solid curve. This dark cluster has a core radius of 0.0042 pc and a central density of $4 \times 10^{12} M_{\odot} \text{ pc}^{-3}$. [This figure is updated from Genzel *et al.* 1997, *M. N. R. A. S.*, **291**, 219 and was kindly provided by R. Genzel.]

4. BH DEMOGRAPHICS

The census of BH candidates as of January 2000 is given in Table 1. The table is divided into three groups – detections based on stellar dynamics, on ionized gas dynamics, and on maser disk dynamics (top to bottom). The rate of discovery is accelerating as *HST* pursues the search. However, we already have candidates that span the range of predicted masses and that occur in essentially every type of galaxy that is expected to contain a BH. Host galaxies include giant AGN ellipticals (the middle group), Seyfert galaxies (NGC 1068), normal spirals with moderately active nuclei (e. g., NGC 4594 and NGC 4258), galaxies with exceedingly weak nuclear activity (our Galaxy and M 31), and completely inactive galaxies (M 32 and NGC 3115).

Table 1 Census of Black Hole Candidates

Galaxy	Type	D (Mpc)	$M_{B,\text{bulge}}$	M_{\bullet} (M_{\odot})	$\log \frac{M_{\bullet}}{M_{\text{bulge}}}$
Galaxy	Sbc	0.0085	−17.65	3×10^6	−3.62
M 31	Sb	0.7	−18.82	3×10^7	−3.31
M 32	E	0.7	−15.51	3×10^6	−2.27
NGC 3115	S0/	8.4	−19.90	1×10^9	−1.92
NGC 4594	Sa/	9.2	−21.21	1×10^9	−2.69
NGC 3377	E	9.9	−18.80	8×10^7	−2.24
NGC 3379	E	9.9	−19.79	1×10^8	−2.96
NGC 4342	S0	15.3	−17.04	3×10^8	−1.64
NGC 4486B	E	15.3	−16.66	6×10^8	−1.03
M 87	E	15.3	−21.42	3×10^9	−2.32
NGC 4374	E	15.3	−20.96	1×10^9	−2.53
NGC 4261	E	29.	−20.89	5×10^8	−2.92
NGC 7052	E	59.	−21.31	3×10^8	−3.31
NGC 6251	E	106.	−21.81	6×10^8	−3.18
NGC 4945	Scd/	3.7	−15.1	1×10^6	...
NGC 4258	Sbc	7.5	−17.3	4×10^7	−2.05
NGC 1068	Sb	15.	−18.8	1×10^7	...

Notes to Table 1: Column 1: galaxy name; column 2: Hubble type; / means that the galaxy is edge-on; column 3: distance based on a Hubble constant of $80 \text{ km s}^{-1} \text{ Mpc}^{-1}$; column 4: absolute B -band magnitude of the bulge component of the galaxy; column 5: BH mass based on isotropic models; column 6: ratio of BH mass to bulge mass. The mass in stars is calculated from the luminosity via the mass-to-light ratio measured at large radii.

However, no complete sample has been studied at high resolution. The detections in Table 1, together with low-resolution studies of larger samples of galaxies, support the hypothesis that BHs live in virtually every galaxy with a substantial bulge component. The total mass in detected remnants is consistent with predictions based on AGN energetics, within the rather large estimated errors in both quantities.

The main new demographic result is an apparent correlation between BH mass and the luminosity of the bulge part of the galaxy. This is shown in Figure 6. Note that the correlation is not with the total luminosity: if the disk is included, the correlation is considerably worse. Whether the correlation is real or not is still being tested. The concern is selection effects. High-mass BHs in small galaxies are easy to see, so their scarcity is real. But low-mass BHs can hide in giant galaxies, so the correlation may be only the upper envelope of a distribution that extends to smaller M_{\bullet} . If it is real, then the correlation implies that BH formation or feeding is connected with the mass of the high-density, elliptical-galaxy-like part of the galaxy. With the possible exception of NGC 4945 (a late-type galaxy for which the existence and luminosity of a bulge are uncertain), BHs have been found only in the presence of a bulge. However, the limits on M_{\bullet} in bulgeless galaxies like M 33 are still consistent with the correlation. Current searches concentrate on the question of whether small BHs – ones that are significantly below the apparent correlation – can be found or excluded.

BH mass fractions are listed in Table 1 for cases in which the mass-to-light ratio of the stars has been measured. The median BH mass fraction is 0.29 %. The quartiles are 0.07 % and 0.9 %.

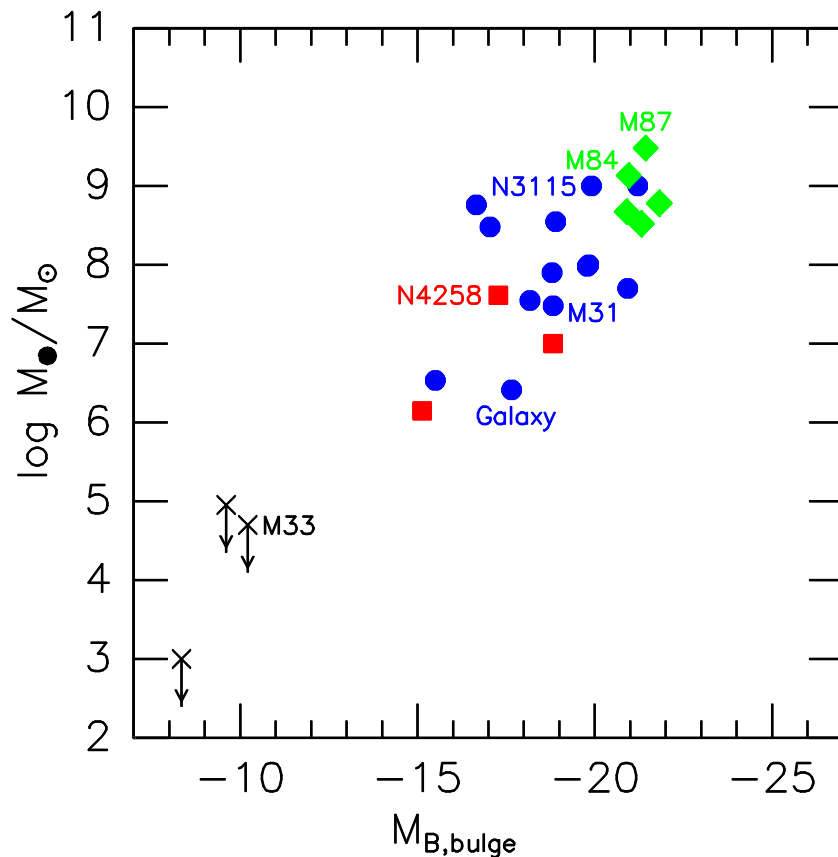


Figure 6. Correlation of BH mass with the absolute magnitude of the bulge component of the host galaxy. Since M/L varies little from bulge to bulge, this implies a correlation between BH mass and bulge mass. Blue filled circles indicate M_{\bullet} measurements based on stellar dynamics, green diamonds are based on ionized gas dynamics, and red squares are based on maser disk dynamics. It is reassuring that all three techniques are consistent with the same correlation.

5. ARE THEY REALLY BLACK HOLES?

The discovery of dark objects with masses $M_{\bullet} \simeq 10^6$ to $10^{9.5} M_{\odot}$ in galactic nuclei is secure. But are they BHs? Proof requires measurement of relativistic velocities near the Schwarzschild radius, $r_s \simeq 2 M_{\bullet}/(10^8 M_{\odot})$ AU. Even for M31, $r_s \sim 8 \times 10^{-7}$ arcsec. *HST* spectroscopic resolution is only $0''.1$. The conclusion that we are finding BHs is based on physical arguments that BH alternatives fail to explain the masses and high densities of galactic nuclei.

The most plausible BH alternatives are clusters of dark objects produced by ordinary stellar evolution. These come in two varieties, failed stars and dead stars. Failed stars have masses $m_* \lesssim 0.08 M_{\odot}$. They never get hot enough for the fusion reactions that power stars, i.e., the conversion of hydrogen to helium. They have a brief phase of modest brightness while they live off of gravitational potential energy, but after this, they could be used to make dark clusters. They are called brown dwarf stars, and they include planetary mass objects. Alternatively, a dark cluster could be made of stellar remnants – white dwarfs, which have typical masses of $0.6 M_{\odot}$; neutron stars, which typically have masses of $\sim 1.4 M_{\odot}$, and black holes with masses of several M_{\odot} . Galactic bulges are believed to form in violent starbursts, so massive stars that turn quickly into dark remnants would be no surprise. It is not clear how one could make dark clusters with the required masses and sizes, especially not without polluting the remaining stars with more metals than we see. But in the absence of direct proof that the dark objects in galactic nuclei are BHs, it is important to examine alternatives.

However, dynamical measurements tell us more than the mass of a potential BH. They also constrain the maximum radius inside which the dark stuff must live. Its minimum density must therefore be high, and this rules out the above BH alternatives in our Galaxy and in NGC 4258. High-mass remnants such as white dwarfs, neutron stars, and stellar BHs would be relatively few in number. The dynamical evolution of star clusters is relatively well understood; in the above galaxies, a sparse cluster of stellar remnants would evaporate completely in $\lesssim 10^8$ yr. Low-mass objects such as brown dwarfs would be so numerous that collision times would be short. Stars generally merge when they collide. A dark cluster of low-mass objects would become luminous because brown dwarfs would turn into stars.

More exotic BH alternatives are not ruled out by such arguments. For example, the dark matter that makes up galactic halos and that accounts for most of the mass of the Universe may in part be elementary particles that are cold enough to cluster easily. It is not out of the question that a cluster of these could explain the dark objects in galaxy centers without getting into trouble with any astrophysical constraints. So the BH case is not rigorously proved. What makes it compelling is the combination of dynamical evidence and the evidence from AGN observations. This is discussed in the previous article.

For many years, AGN observations were decoupled from the dynamical evidence for BHs. This is no longer the case. Dynamical BH detections are routine. The search itself is no longer the main preoccupation; we can concentrate on physical questions. New technical developments such as better X-ray satellites ensure that progress on BH astrophysics will continue to accelerate.

6. SUGGESTIONS FOR FURTHER READING

- The search for BHs is reviewed in the following papers:
Kormendy, J., & Richstone, D. *Ann. Rev. Astr. Astrophys.* **33**, 581 (1995)
Richstone, D., *et al.* *Nature* **395**, A14 (1998)
- In the following papers, quasar energetics are used to predict the masses of dead AGN engines:
Sołtan, A. *M.N.R.A.S.* **200**, 115 (1982)
Chokshi, A., & Turner, E. L. *M.N.R.A.S.* **259**, 421 (1992)
- Dynamical models of galaxies as linear combinations of individual orbits are discussed in
Schwarzschild, M. *Astrophys. J.* **232**, 236 (1979)
Richstone, D. O., & Tremaine, S. *Astrophys. J.* **327**, 82 (1988)
van der Marel, R. P., Cretton, N., de Zeeuw, P. T., & Rix, H.-W. *Astrophys. J.* **493**, 613 (1998)
Gebhardt, K., *et al.* *Astron. J.* **119**, 1157 (2000)
- The BH detection in NGC 3115 is discussed in
Kormendy, J., & Richstone, D. *Astrophys. J.* **393**, 559 (1992)
Kormendy, J., *et al.* *Astrophys. J. Lett.* **459**, L57 (1996)
- The BH detection in M 31 is discussed in
Dressler, A., & Richstone, D. O. *Astrophys. J.* **324**, 701 (1988)
Kormendy, J. *Astrophys. J.* **325**, 128 (1988)
- Tremaine's model for the double nucleus of M 31 and new evidence for that model are in
Tremaine, S. *Astron. J.* **110**, 628 (1995)
Kormendy, J., & Bender, R. *Astrophys. J.* **522**, 772 (1999)
- *HST* spectroscopy of the double nucleus of M 31 is presented in
Statler, T. S., King, I. R., Crane, P., & Jędrzejewski, R. I. *Astron. J.* **117**, 894 (1999)
- The following are thorough reviews of the Galactic center:
Genzel, R., Hollenbach, D., & Townes, C. H. *Rep. Prog. Phys.* **57**, 417 (1994)
Morris, M., & Serabyn, E. *Ann. Rev. Astr. Astrophys.* **34**, 645 (1996)
- The latest measurement of the size of the Galactic center radio source is by
Lo, K. Y., Shen, Z.-Q., Zhao, J.-H., & Ho, P. T. P. *Astrophys. J. Lett.* **508**, L61 (1998)
- The remarkable proper motion measurements of stars near Sgr A* and resulting conclusions about the Galactic center BH are presented in
Genzel, R., Eckart, A., Ott, T., & Eisenhauer, F. *M.N.R.A.S.* **291**, 219 (1997)
Ghez, A. M., Klein, B. L., Morris, M., & Becklin, E. E. *Astrophys. J.* **509**, 678 (1998)

- Arguments against compact dark star clusters in NGC 4258 and the Galaxy are presented in Maoz, E. *Astrophys. J. Lett.* **494**, L181 (1998)